



# Synthesis, biological evaluation, theoretical investigations, docking study and ADME parameters of some 1,4-bisphenylhydrazone derivatives as potent antioxidant agents and acetylcholinesterase inhibitors

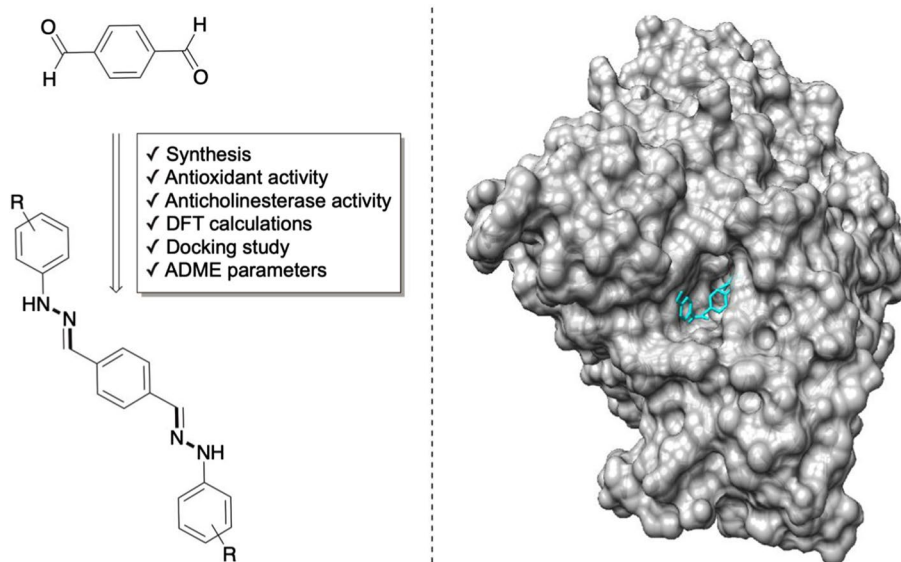
Imene Amine Khodja<sup>1</sup> · Housseem Boulebd<sup>1</sup>

Received: 22 December 2019 / Accepted: 26 February 2020  
© Springer Nature Switzerland AG 2020

## Abstract

Five 1,4-bisphenylhydrazone derivatives (**1–5**) were successfully synthesized and evaluated for their antioxidant and acetylcholinesterase inhibitory activities. The antioxidant activity has been carried out using DPPH, ABTS, CUPRAC and superoxide radical scavenging methods. All the compounds showed a very good antioxidant activity compared to that of the standards used. Compound **1** was found to be the best antioxidant agent with  $IC_{50}$  values lower or comparable to that of the standards. The acetylcholinesterase inhibitory activity has been evaluated using a modified Ellman's assay. The obtained results indicate that compound **2** is the best acetylcholinesterase inhibitor with a low  $IC_{50}$  value comparable to that of the galantamine. In addition, DFT calculations have been performed to determine in which mechanism the synthesized hydrazones follow to scavenge free radicals. Molecular docking study was performed for compound **2**, and its interaction modes with the enzyme acetylcholinesterase were determined. As a result, a strong interaction between this compound and the active site of AChE enzyme was revealed. Finally, ADME properties of the synthesized compounds were also studied and showed good drug-like properties.

## Graphic abstract



**Electronic supplementary material** The online version of this article (<https://doi.org/10.1007/s11030-020-10064-8>) contains supplementary material, which is available to authorized users.

Extended author information available on the last page of the article

**Keywords** Hydrazone · Acetylcholinesterase · Antioxidant activity · Docking study · DFT calculations · ADME parameters

## Introduction

Hydrazone is an azomethine group characterized by the triatomic structure C=N–N. This functional group can be obtained by simple condensation between hydrazine or its derivatives and aldehydes or ketones. The presence of specific functionalities at the hydrazine or the carbonyl compound promotes the formation of very attractive systems such as chemosensors [1, 2], adsorbents [3], dyes [4, 5] and catalysts [6]. Molecules derived from hydrazone present a wide range of biological activities such as anticancer [7], antimicrobial [8, 9], anti-inflammatory [10], antifungal [11], antitubercular [12] and antiviral [13]. Hydrazone functional group is present also in a number of anticancer, antifungal, antibiotic and antihypertensive commercial drugs such as mitoguzone, ferimzone, nifuroxazide and dihydralazine (Fig. 1).

Hydrazone-based compounds are widely studied for their antioxidant properties, and several studies have shown that this family of compounds has high antioxidant activity [14–17]. In the medicinal point of view, compounds with potent antioxidant properties are very attractive candidates for drug development, because the oxidative stress is well known to be involved in several human diseases such as cancer, Parkinson's disease, Alzheimer's disease,

atherosclerosis, myocardial infarction, sickle cell disease, vitiligo, autism and others [18, 19].

Although the antioxidant properties of compounds derived from hydrazone functional group have been widely studied, few works describe a fundamental theoretical study of the structure–activity relationship of these compounds [20, 21]. The main aim of this research work is the synthesis and the study of the antioxidant properties of a series of aryl compounds bearing two hydrazone functions in one molecule. Firstly, the antioxidant activity has been evaluated *in vitro* by using series of assays including DPPH (2,2-diphenyl-1-picrylhydrazyl), ABTS (2,2'-azino-bis(3-ethylbenzothiazoline-6-sulfonic acid), CUPRAC (cupric ion reducing antioxidant capacity) and DMSO alkaline. Then, a theoretical study based on DFT (density functional theory) calculations for the most active compound has been carried out in order to better understand the antioxidant activity of this family of compounds. Antioxidant mechanisms, frontier molecular orbitals and molecular electrostatic potential (MEP) mapping have been investigated. To further explore the multifunctional properties of the synthesized hydrazones, their acetylcholinesterase inhibitory activity has been also investigated. This enzyme is a primary target for symptomatic improvement in Alzheimer's disease [22]. The obtained experimental results were validated by molecular docking study. Finally, *in silico* ADME (absorption, distribution, metabolism and excretion) parameters of all the compounds have been determined to evaluate their pharmacokinetic properties.

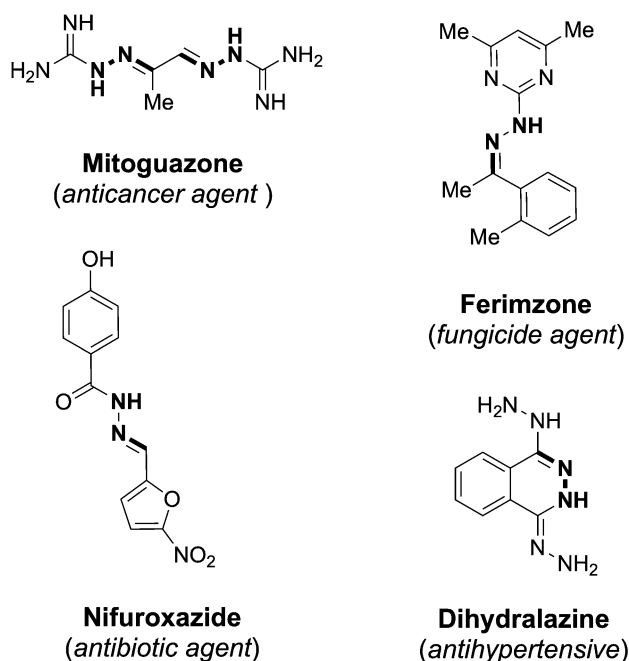


**Fig. 1** Some commercial drugs derived from hydrazone scaffold

## Experimental section

### Materials and instrumentation

The FTIR spectra were recorded with a JASCO FT/IR-6300 type A spectrometer, and only significant absorption band frequencies are cited. <sup>1</sup>H NMR and <sup>13</sup>C NMR spectra were recorded on a Bruker Avance DPX250. Melting points were determined on a Kofler melting point apparatus. Commercial-grade reagents were used as supplied: terephthalaldehyde 98% (Alfa Aesar), phenylhydrazine 97% (Alfa Aesar), 4-chlorophenylhydrazine 97% (Alfa Aesar), 4-methoxyphenylhydrazine 99% (Alfa Aesar), 3,4-dimethylphenylhydrazine 98% (Alfa Aesar), [4-(benzyloxy)phenyl]hydrazine 98% (Alfa Chemistry).

## General procedure for the synthesis of 1,4-bisphenylhydrazone derivatives 1–5

In a 25-mL Erlenmeyer flask, 1 mmol of terephthalaldehyde and 2 mmol of phenylhydrazine derivative were dissolved in 3 ml of ethanol. The reaction mixture was stirred for 4 h at room temperature; then, it was filtered and air-dried. The resulting residue was then purified by recrystallization in a mixture of ethanol/DMSO to give the pure product.

**1,4-bis((E)-(2-phenylhydrazineylidene)methyl)benzene (1)** Yield: 87%. (Yellow crystals) Mp > 260 °C. IR:  $\nu_{\max}$  1628 (C=N)  $\text{cm}^{-1}$ .  $^1\text{H}$  NMR (250 MHz, DMSO-*d*6):  $\delta$  10.53 (brs, 2H, NH), 7.90–7.87 (m, 2H,  $\text{H}_{\text{aromatic}}$ ), 7.69–7.66 (m, 4H,  $2\text{H}_{\text{aromatic}}$ ,  $2\text{CH}_{\text{imine}}$ ), 7.24 (t, 4H,  $J=7.4$  Hz,  $\text{H}_{\text{aromatic}}$ ), 7.12–7.04 (m, 4H,  $\text{H}_{\text{aromatic}}$ ), 6.80–6.74 (m, 2H,  $\text{H}_{\text{aromatic}}$ ).  $^{13}\text{C}$  NMR (62.5 MHz, DMSO-*d*6):  $\delta$  145.20, 136.18, 135.35, 129.20, 125.92, 118.85, 112.04.

**1,4-bis((E)-(2-(4-methoxyphenyl)hydrazineylidene)methyl)benzene (2)** Yield: 85%. (Yellow crystals) Mp = 259 °C. IR:  $\nu_{\max}$  1642 (C=N)  $\text{cm}^{-1}$ .  $^1\text{H}$  NMR (250 MHz, DMSO-*d*6):  $\delta$  10.21 (brs, 2H, NH), 7.90 (s, 2H,  $\text{CH}_{\text{imine}}$ ), 7.38–7.31 (m, 2H,  $\text{H}_{\text{aromatic}}$ ), 7.24–7.18 (m, 2H,  $\text{H}_{\text{aromatic}}$ ), 7.17–7.08 (m, 4H,  $\text{H}_{\text{aromatic}}$ ), 7.04–6.96 (m, 4H,  $\text{H}_{\text{aromatic}}$ ), 3.76 (s, 6H, OMe).  $^{13}\text{C}$  NMR (62.5 MHz, DMSO-*d*6):  $\delta$  142.04, 141.08, 129.17, 129.07, 124.36, 123.76, 122.91, 122.47, 121.60, 114.34, 113.98, 35.63.

**1,4-bis((E)-(2-(3,4-dimethylphenyl)hydrazineylidene)methyl)benzene (3)** Yield: 91%. (Yellow crystals) Mp > 260 °C. IR:  $\nu_{\max}$  1633 (C=N)  $\text{cm}^{-1}$ .  $^1\text{H}$  NMR (250 MHz, DMSO-*d*6):  $\delta$  10.36 (brs, 2H, NH), 7.82–7.79 (m, 2H,  $\text{H}_{\text{aromatic}}$ ), 7.63–7.62 (m, 4H,  $2\text{H}_{\text{aromatic}}$ ,  $2\text{CH}_{\text{imine}}$ ), 7.00–6.81 (m, 6H,  $\text{H}_{\text{aromatic}}$ ), 2.20 (s, 3H, Me), 2.14 (s, 3H, Me).  $^{13}\text{C}$  NMR (62.5 MHz, DMSO-*d*6):  $\delta$  143.28, 136.74, 135.38, 135.33, 130.14, 126.26, 125.77, 113.41, 109.58, 19.88, 18.67.

**1,4-bis((E)-(2-(4-chlorophenyl)hydrazineylidene)methyl)benzene (4)** Yield: 89%. (Yellow crystals) Mp > 260 °C. IR:  $\nu_{\max}$  1625 (C=N), 680 (C–Cl)  $\text{cm}^{-1}$ .  $^1\text{H}$  NMR (250 MHz, DMSO-*d*6):  $\delta$  10.58 (brs, 2H, NH), 7.93–7.87 (m, 2H,  $\text{H}_{\text{aromatic}}$ ), 7.74–7.66 (m, 4H,  $2\text{H}_{\text{aromatic}}$ ,  $2\text{CH}_{\text{imine}}$ ), 7.28–7.25 (m, 4H,  $\text{H}_{\text{aromatic}}$ ), 7.11–7.03 (m, 4H,  $\text{H}_{\text{aromatic}}$ ).  $^{13}\text{C}$  NMR (62.5 MHz, DMSO-*d*6):  $\delta$  144.14, 137.04, 135.33, 129.04, 126.11, 122.11, 113.5.

**1,4-bis((E)-(2-(4-benzyloxyphenyl)hydrazineylidene)methyl)benzene (5)** Yield: 94%. (Yellow crystals) Mp = 258 °C. IR:  $\nu_{\max}$  1632 (C=N)  $\text{cm}^{-1}$ .  $^1\text{H}$  NMR (250 MHz, DMSO-*d*6):  $\delta$  10.30 (brs, 2H, NH), 7.81–7.80 (m, 2H,  $\text{H}_{\text{aromatic}}$ ), 7.62–7.60 (m, 4H,  $2\text{H}_{\text{aromatic}}$ ,  $2\text{CH}_{\text{imine}}$ ), 7.47–7.32 (m, 8H,  $\text{H}_{\text{aromatic}}$ ),

7.06–7.02 (m, 4H,  $\text{H}_{\text{aromatic}}$ ), 6.96–6.92 (m, 4H,  $\text{H}_{\text{aromatic}}$ ), 4.95 (s, 4H,  $\text{H}_{\text{benzylic}}$ ).  $^{13}\text{C}$  NMR (62.5 MHz, DMSO-*d*6):  $\delta$  151.71, 139.51, 137.55, 135.29, 135.17, 128.42, 127.72, 125.70, 119.41, 115.81, 112.99, 69.66.

## In vitro antioxidant evaluation

### DPPH free radical scavenging assay

The free radical scavenging activity was determined spectrophotometrically by the DPPH assay [23]. In its radical form, DPPH absorbs at 517 nm, but upon reduction by an antioxidant or a radical species its absorbance decreases. Briefly, a 0.1 mM solution of DPPH in ethanol was prepared and 4 mL of this solution was added to 1 mL of sample solutions in ethanol at different concentrations (3.12, 6.25, 12.5, 25, 50, 100 and 200  $\mu\text{M}$ ). Thirty minutes later, the absorbance was measured at 517 nm. Lower absorbance of the reaction mixture indicated higher free radical scavenging activity. BHT and BHA, under the same conditions as the samples and for each concentration, were used as antioxidant standards. The DPPH radical scavenging activity was calculated using the following equation:

$$\text{DPPH scavenging effect (\%)} = \frac{A_{\text{Control}} - A_{\text{Sample}}}{A_{\text{Control}}} \times 100$$

where  $A_{\text{control}}$  and  $A_{\text{sample}}$  are the absorbances of the reference and sample obtained from the UV–visible spectrophotometer, respectively. The results were given as  $\text{IC}_{50}$  ( $\mu\text{M}$ ) corresponding to the concentration of 50% of inhibition.

### ABTS radical scavenging assay

The ABTS<sup>+</sup> scavenging activity was determined according to the method of Re et al. [24]; 10  $\mu\text{L}$  aliquot of each tested sample at different concentrations (3.12, 6.25, 12.5, 25, 50, 100 and 200  $\mu\text{M}$ ) was added to 1.0 mL of diluted ABTS<sup>+</sup> solution. The ABTS<sup>+</sup> was generated by the reaction between 7 mM ABTS in water and 2.45 mM potassium persulfate and stored in the dark at room temperature for 12 h. The ABTS<sup>+</sup> solution was diluted to get an absorbance of  $0.703 \pm 0.025$  at 734 nm with ethanol which was used as a control. After 10 min, the absorbance was measured at 734 nm. BHT and BHA, under the same conditions as the samples and for each concentration, were used as antioxidant standards. The ABTS radical scavenging activity was calculated using the following equation:

$$\text{ABTS scavenging effect (\%)} = \frac{A_{\text{Control}} - A_{\text{Sample}}}{A_{\text{Control}}} \times 100$$

where  $A_{\text{control}}$  and  $A_{\text{sample}}$  are the absorbances of the reference and sample obtained from the UV–visible spectrophotometer, respectively. The results were given as  $IC_{50}$  ( $\mu\text{M}$ ) corresponding to the concentration of 50% of inhibition.

#### Cupric reducing antioxidant capacity (CUPRAC) assay

The cupric reducing capacity of the compounds was determined by the CUPRAC method [25]. One milliliter of copper (II) chloride solution (0.01 M prepared from  $\text{CuCl}_2 \cdot 2\text{H}_2\text{O}$ ), 1 mL of ammonium acetate buffer at pH 7.0 and 1 mL of neocuproine solution (0.0075 M) were mixed to 0.5 mL of samples or standard of different concentration solutions (3.12, 6.25, 12.5, 25, 50, 100 and 200  $\mu\text{M}$ ). The final volume of the mixture was adjusted to 4.1 mL by adding 0.6 mL of distilled water. The resulting mixture was incubated for 1 h at room temperature, and then, the absorbance of the solution was measured at 450 nm by the use of a spectrophotometer against blank and BHT and BHA as standards. The results were given as  $A_{0.5}$  ( $\mu\text{M}$ ) corresponding the concentration indicating 0.50 absorbance intensity.

#### Superoxide radical scavenging activity (DMSO alkaline assay)

Superoxide was generated according to the alkaline DMSO method described by Hyland et al. [26]. Superoxide radical ( $\text{O}_2^-$ ) is generated by the addition of sodium hydroxide to air-saturated DMSO. The generated superoxide remains stable in solution and reduces nitroblue tetrazolium (NBT) into formazan dye at room temperature which can be measured at 560 nm. The final volume used (1.4 mL) for the absorbance measurement was 0.1 mL of NBT (1 mg/mL) was added to the reaction mixture containing 1 mL of alkaline DMSO (1 mL DMSO containing 5 mM NaOH in 0.1 mL water) and 0.3 mL of the tested sample at various concentrations (3.12, 6.25, 12.5, 25, 50, 100 and 200  $\mu\text{M}$ ). Tocopherol (TOC) and tannic acid (TAC) were used as positive control. The results were given as  $IC_{50}$  ( $\mu\text{M}$ ) corresponding to the concentration of 50% of inhibition.

#### Inhibition of acetylcholinesterase

AChE inhibitory activity was measured using quantitative colorimetric assay using a 96-well microplate reader according to the method described by Rhee et al. [27] based on Ellman's method [28]. The enzyme hydrolyzes the substrate acetylthiocholine resulting in the product thiocholine which reacts with Ellman's reagent: 5,5'-dithiobis(2-nitrobenzoic acid) (DTNB) to produce

2-nitrobenzoic-5-mercaptothiocholine and 5-thio-2-nitrobenzoate which can be detected at 412 nm. In this method, 150  $\mu\text{L}$  of 100 mM sodium phosphate buffer (pH 8.0), 10  $\mu\text{L}$  of test solution at different concentrations (3.12, 6.25, 12.5, 25, 50, 100 and 200  $\mu\text{M}$ ) and 20  $\mu\text{L}$  of AChE from *Electrophorus electricus* ( $5.32 \times 10^{-3}$  units) solutions were mixed and incubated for 15 min at 25 °C, and 10  $\mu\text{L}$  of 0.5 mM (DTNB) was added. The reaction was then initiated by the addition of 10  $\mu\text{L}$  of acetylthiocholine iodide (0.71 mM). The hydrolysis of this substrate was monitored spectrophotometrically at a wavelength of 412 nm, every 5 min for 15 min in triplicate experiments. The results were given as  $IC_{50}$  ( $\mu\text{M}$ ), and the percentage of inhibition was determined by the comparison of reaction rates of samples relative to the blank sample (methanol in phosphate buffers, pH 8) using the formula:

$$\text{Percentage of inhibition (\%)} = \frac{A_{\text{Control}} - A_{\text{Sample}}}{A_{\text{Control}}} \times 100$$

where  $A_{\text{control}}$  and  $A_{\text{sample}}$  are the absorbances of the reference and sample obtained from the UV–visible spectrophotometer, respectively.

#### Computational details

Density functional theory (DFT) calculations have been carried out using Gaussian09 software [29]. The B3LYP functional [30, 31] and the 6-311G(d,p) basis set have been used for all calculations. This approach has been used successfully by several research groups, and good agreement between theory and experiment was found [32–36]. Solvent effect of ethanol was approximated by the integral equation formalism of polarizable continuum model (IEF-PCM). All the ground states were confirmed by vibrational frequency analysis (no imaginary frequency). The numerical descriptors of the antioxidant mechanisms (**BDE**, **IE**, **PDE**, **PA**, **ETE**) have been calculated as follows [37–39]:

$$\text{BDE} = H(\text{R}^\cdot) + H(\text{H}) - H(\text{R} - \text{H})$$

$$\text{IE} = H(\text{RH}^+) + H(e^-) - H(\text{R} - \text{H})$$

$$\text{PDE} = H(\text{R}^\cdot) + H(\text{H}^+) - H(\text{RH}^+)$$

$$\text{PA} = H(\text{R}^-) + H(\text{H}^+) - H(\text{R} - \text{H})$$

$$\text{ETE} = H(\text{R}^\cdot) + H(e^-) - H(\text{R}^-)$$

where  $H(R^\cdot)$  is the enthalpy obtained by geometry optimization of the radicals formed after abstracting of H atom from the NH bond,  $H(H^\cdot)$  is the enthalpy of a single H atom at the B3LYP/6-311G(d,p) level,  $H(R-H)$  is the enthalpy of the neutral molecule,  $H(RH^+)$  is the enthalpy of radical cation.  $H(e^-)$  is the enthalpy of single electron,  $H(H^+)$  is the enthalpy of proton, and  $H(R^-)$  is the enthalpy of charged molecule after abstracting of a proton from the NH bond. The calculated enthalpies of the hydrogen (H), electron ( $e^-$ ) and proton ( $H^+$ ) in gas phase and solvent environment were taken from the literature [40–44].

## Molecular docking study

In order to investigate the possible binding modes of compound **2** (the most active compound) to the protein AChE, calculations were carried out with “Achilles” Blind Docking server, available at: <http://bio-hpc.eu/>. Using a “blind docking” approach, the docking of the small molecule to the targets is carried out without a priori knowledge of the location of the binding site by the system [45]. Figures were drawn using the Chimera program [46]. The ligand structures have been built and energy-minimized using the program Marvin-Sketch [ChemAxon Ltd, Budapest, Hungary]. The coordinates of AChE (PDB ID: 1C2B) were obtained from the Protein Data Bank (PDB).

## ADME parameters and BBB permeability

ADME properties were predicted using Molinspiration online property calculation toolkit available at: <http://www.molinspiration.com>. The BBB permeability was evaluated by using the CBLigand-BBB prediction server available at: <http://www.cbligand.org>.

## Results and discussion

### Chemistry

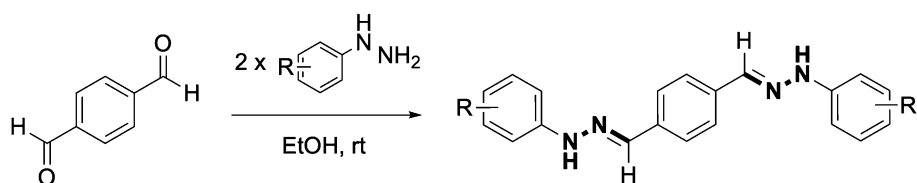
The 1,4-bisphenylhydrazone derivatives were easily prepared from terephthalaldehyde and phenylhydrazine derivatives as presented in Scheme 1. The reaction of one equivalent of terephthalaldehyde with two equivalents of phenylhydrazine derivative (phenylhydrazine, 4-methoxyphenylhydrazine, 3,4-dimethylphenylhydrazine, 4-chlorophenylhydrazine and (4-benzylphenyl)hydrazine) at room temperature for 4 h in ethanol gives the corresponding 1,4-bisphenylhydrazone derivatives **1–5** in excellent yields (85–94%). The molecular structures of the synthesized compounds were confirmed by IR,  $^1H$  NMR and  $^{13}C$  NMR spectroscopies.

### Antioxidant activity

#### In vitro investigation of the antioxidant activity

The antioxidant activity of the synthesized hydrazones was evaluated using a series of assays. Firstly, assays based on two oxidants, the radical 2,2-diphenyl-1-picrylhydrazyl (DPPH) and the radical cation 2,20-azino-bis-(3-ethylbenzothiazoline-6-sulfonic acid ( $ABTS^{\cdot+}$ ), have been used to evaluate the radical scavenging properties of the synthesized compounds. In these assays, the total antioxidant activity of a molecule is deduced from its ability to inhibit the DPPH or  $ABTS^{\cdot+}$  radicals [47]. DMSO alkaline assay has been used to evaluate the potential of the investigated molecules to scavenge superoxide radical. In this method, the antioxidant reacts with  $O_2^-$  to generate the stable  $O_2$  molecule [26]. Finally, the cupric ion reducing capability has been

**Scheme 1** Synthesis and structures of 1,4-bisphenylhydrazone derivatives (**1–5**)



Comp.	R
<b>1</b>	H
<b>2</b>	4-OMe
<b>3</b>	3,4-diMe
<b>4</b>	4-Cl
<b>5</b>	4-OCH <sub>2</sub> Ph

elucidated by CUPRAC assay. This method measures the ability of an antioxidant to reduce  $\text{Cu}^{2+}$  to  $\text{Cu}^+$  [48]. Butylated hydroxytoluene (BHT) and butylated hydroxyanisole (BHA) were used as positive controls for DPPH, ABTS and CUPRAC assays and  $\alpha$ -tocopherol (TOC) and tannic acid (TAC) for DMSO alkaline assay. The  $\text{IC}_{50}$  and  $A_{0.50}$  values were determined for all compounds and are reported in Fig. 2 and Table S1 in SI.

An examination of DPPH, ABTS, CUPRAC and DMSO alkaline assays results, as shown in Fig. 2 and Table S1, reveals the following observations: All the tested compounds 1–5 exhibited a high antioxidant activity when compared to the standards with  $\text{IC}_{50}$  and  $A_{0.50}$  values  $< 72.27 \pm 0.46 \mu\text{M}$ . In DPPH assay, all the studied compounds have shown a higher antiradical activity than the standard BHT ( $\text{IC}_{50}$ :  $19.90 \pm 0.51$ – $68.55 \pm 1.74$  vs  $81.29 \pm 1.19 \mu\text{M}$ ). Compound 1 followed by compound 3 is the best antioxidant agents with  $\text{IC}_{50}$  values ( $26.75 \pm 0.05 \mu\text{M}$  and  $30.12 \pm 1.20 \mu\text{M}$ , respectively) about three times less than that of the BHT ( $81.29 \pm 1.19 \mu\text{M}$ ) and comparable to that of the BHA ( $31.79 \pm 0.41 \mu\text{M}$ ). Compounds 4 ( $\text{IC}_{50} = 40.08 \pm 0.54 \mu\text{M}$ ) and 5 ( $\text{IC}_{50} = 39.90 \pm 0.51 \mu\text{M}$ ) have comparable  $\text{IC}_{50}$  values slightly higher than that of the BHA ( $31.79 \pm 0.41 \mu\text{M}$ ). Among the studied compound, the least reactive antioxidant was found to be compound 2 with an  $\text{IC}_{50}$  value of  $68.55 \pm 1.74 \mu\text{M}$ . The antioxidant activity of compounds 1–5 in DPPH assay can be ranked in the order:  $1 > 3 > 5 > 4 > 2$ . In ABTS assay, the same order was observed, and the best result was obtained with compound 1, which shows an  $\text{IC}_{50}$  value ( $9.76 \pm 0.07 \mu\text{M}$ ) lower than that of the BHT and BHA ( $15.85 \pm 0.30$  and  $10.04 \pm 0.10 \mu\text{M}$ , respectively). In DMSO alkaline assay, the best results were observed with compounds 1 and 4, and these compounds have shown a higher antioxidant activity than the standards TAA ( $9.71 \pm 0.16 \mu\text{M}$ ) and TOC ( $24.36 \pm 0.86 \mu\text{M}$ ) with  $\text{IC}_{50}$  values of  $5.38 \pm 0.21 \mu\text{M}$  and  $7.67 \pm 0.68 \mu\text{M}$ , respectively. The

order of the antioxidant activity by DMSO alkaline assay is  $1 > 4 > 5 > 2 > 3$ . Finally, in CUPRAC assay compound 1 has shown the best result with  $A_{0.50}$  value ( $30.12 \pm 0.81 \mu\text{M}$ ) slightly lower than that of the BHT ( $43.66 \pm 0.87 \mu\text{M}$ ) and slightly higher than that of the BHA ( $20.19 \pm 0.19 \mu\text{M}$ ). The order of the antioxidant activity is  $1 > 3 > 4 > 5 > 2$ .

Overall, among the studied compounds, the hydrazone 1 (non-substituted compound) was found to be the best antioxidant agent. This compound shows a higher or comparable antioxidant activity than BHT and BHA in DPPH, ABTS and CUPRAC assays, as well as a higher antioxidant activity than TOC and TAA in DMSO alkaline assay. On the other hand, compound 2 (bearing methoxy group) was found to be the least reactive antioxidant agent among the synthesized compounds. The other compounds (3–5) have relatively comparable antioxidant activity, especially in DPPH, ABTS and CUPRAC assays. As can be concluded from the obtained results, the synthesized hydrazones 1–5 are antioxidants as potent as the standards BHT, BHA, TAA and TOC. These results are in line with those of other reported hydrazone-based compounds [49–51].

### Theoretical evaluation of radical scavenging mechanisms

It is widely established that antioxidants scavenge free radicals following several mechanisms [52]. The most studied in literature are: hydrogen atom transfer (HAT), sequential electron transfer proton transfer (SETPT) and sequential proton loss electron transfer (SPLET) [36, 53–56]. In the HAT mechanism, hydrogen atom transfers from the antioxidant to the free radical in one step. The SETPT mechanism involves two steps: the initial formation of a radical cation by the transfer of an electron from the antioxidant to the free radical and a proton transfer from the radical cation to the anion. The SPLET mechanism involves the dissociation of a proton from the antioxidant followed by an electron transfer

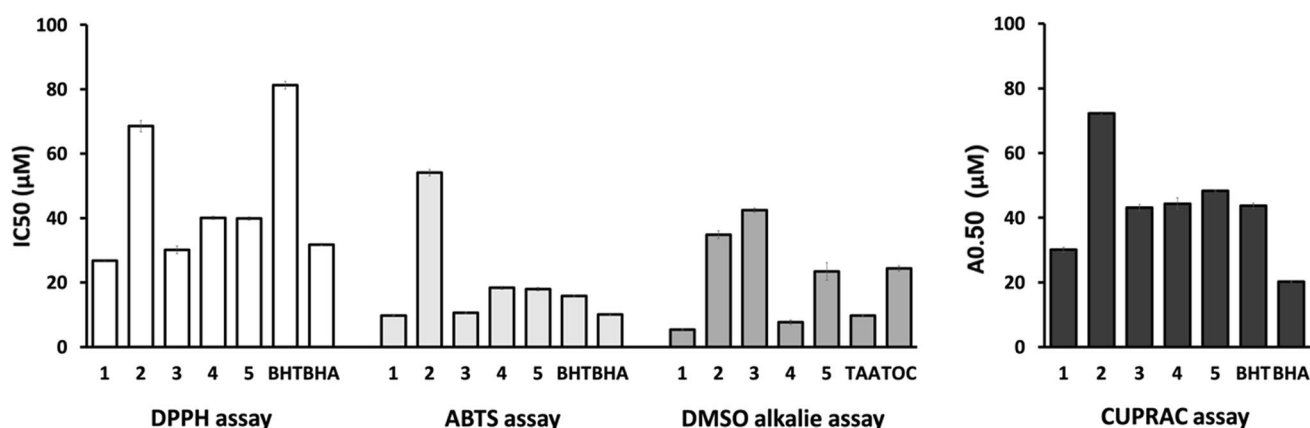


**Fig. 2** Antioxidant activity of compounds 1–5 by DPPH, ABTS, CUPRAC and DMSO alkaline assays. Values expressed are mean  $\pm$  S.D. of three parallel measurements. ( $p < 0.05$ )

to the free radical. The **HAT** mechanism is characterized by the **BDE** (bond dissociation enthalpy) value that corresponds to the ability of an antioxidant to donate its hydrogen atom and consequently form a radical. The lower the **BDE** value, the better the antioxidant properties. The **SETPT** mechanism is characterized by the **IP** (ionization potential) value, which represents the enthalpy required to remove an electron from the neutral molecule and the **PDE** (proton dissociation enthalpy) value that corresponds to the enthalpy of deprotonation of the antioxidant radical cation. The lower the **IP** and **PDE** values, the higher the antioxidant activity. Finally, the **SPLET** mechanism is characterized by the **PA** (proton affinity) value, which corresponds to the enthalpy of the dissociation of a proton from the neutral molecule and the **ETE** (electron transfer enthalpy) value that corresponds to the enthalpy of the transfer of an electron from the antioxidant anion to the free radical. The lower **PA** and **ETE** values are characteristic of higher antioxidant activity.

In order to have a better understanding of the antioxidant properties of the synthesized hydrazones **1–5** and in which mechanism they follow to scavenge free radicals, the three main antioxidant mechanisms (**HAT**, **SETPT** and **SPLET**) have been investigated. Using DFT method at B3LYP/6-311G(d,p) level of theory, we have calculated the numerical descriptors of the antioxidant mechanisms (**BDE**, **IP**, **PDE**, **PA** and **ETE**) for compound **1**, as representative compound, and for BHT for comparison. The implicitly of ethanol has been also considered by employing the integral equation formalism of polarizable continuum model (IEF-PCM). The obtained results are depicted in Fig. 3 and tabulated in Table S2 in SI.

As shown in Fig. 3 and Table S2, both compound **1** and **BHT** have a small **BDE** values ranging from 70.42 to 76.45 kcal/mol, indicating that both O–H and N–H functions are easy to break and form stable radicals. **BDE** values of BHT are about 5 kcal/mol lower than that of compound **1** in the two studied mediums. The **IP** values of compound **1** are about 25 kcal/mol and 15 kcal/mol lower than that of BHT in the gas phase and ethanol, respectively, while the **PDE** values of BHT are lower than that of compound **1** by about 20 kcal/mol and 30 kcal/mol in the gas phase and ethanol, respectively. This indicates that both compound **1** and BHT have a comparable antioxidant activity via **SETPT** mechanism. It should be noted that all the **IP** and **PDE** values are decreased in ethanol by about 60 kcal/mol and 210 kcal/mol, respectively. These decreases are due to the high solvation enthalpies of electron and proton in solution, which is in line with the results from previous studies on phenolic compounds [57, 58].

Compound **1** and BHT have a comparable **PA** and **ETE** values in the studied mediums, indicating that both compounds have also a comparable antioxidant activity via **SPLET** mechanism. As observed with **IP** and **PDE** values,

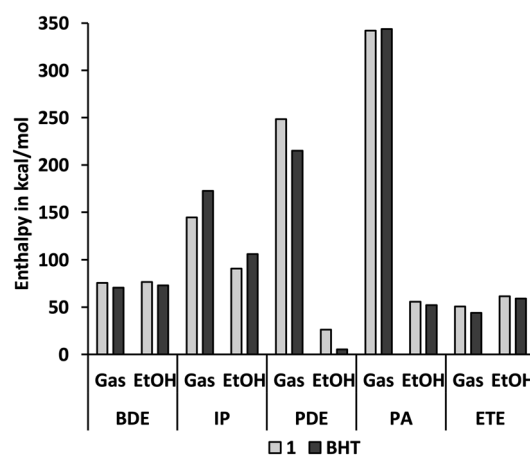


**Fig. 3** Thermodynamic descriptors, **BDE** (bond dissociation enthalpy), **IP** (ionization potential), **PDE** (proton dissociation enthalpy), **PA** (proton affinity) and **ETE** (electron transfer enthalpy), of the antioxidant mechanisms for compound **1** and BHT in the gas phase and EtOH

the **PA** values are dramatically decreased by about 290 kcal/mol in ethanol due to the large solvation enthalpies of the proton. In contrast to **IP**, **PDE** and **PA** values, **ETE** values are slightly increased in ethanol by 10 kcal/mol. These results are also in line with previous studies [54, 59, 60].

Thermodynamically, the antioxidant preferred mechanism can be determined by comparing the **BDE**, **IP** and **PA** values, in which **IP** and **PA** values are related to the first steps of **SETPT** and **SPLET** mechanisms, respectively [57, 61]. As shown in Fig. 3 and Table S2, for both compound **1** and BHT, the **IP** and **PA** values are significantly higher than the **BDE** values in the gas phase, indicating that the **HAT** is the dominate mechanism in this medium. In ethanol, the large decrease observed with **PA** values makes **SPLET** the more favorable mechanism.

It is well known that the energy and distribution of highest occupied molecular orbitals (HOMO) of an antioxidant are correlated with its antioxidant activity [61]. Molecules with lower HOMO energy are less likely to donate electrons [62]. Moreover, the high electronic density of distribution of HOMO determines the sites for the free radical attack. Using the same level of theory as described above, we have calculated the energies and distribution of HOMO orbitals of compound **1** and BHT in the gas phase (Fig. 4). As shown in Fig. 4, the HOMO of compound **1** is delocalized over the whole molecule including the two hydrazone functions, while the HOMO of BHT is only located on the phenol group. In addition, HOMO energy of compound **1** is slightly higher than that of BHT with values of  $-5.07$  eV and  $-5.74$  eV, respectively. This indicates that the electron donating ability of compound **1** is slightly better than that

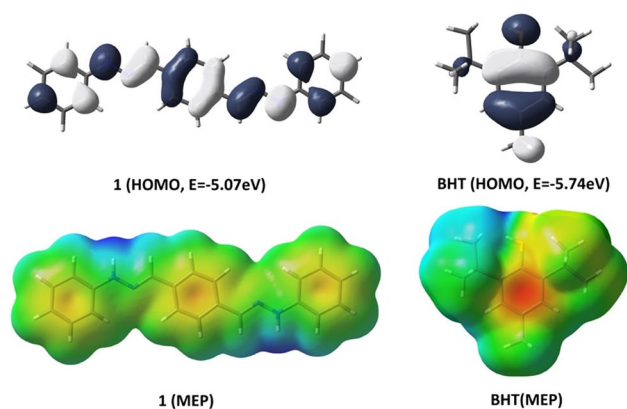


**Fig. 4** HOMO orbital distribution and energy as well as the molecular electrostatic potential (MEP) mapping of compound **1** (left) and BHT (right) in the gas phase

of BHT. These results are in good agreement with the calculated **IP** values.

Molecular electrostatic potential (MEP) mapping is another parameter that characterizes the antioxidant properties of the investigated compounds [33, 63, 64]. The more positive sites are the privileged sites for free radical attack. MEP mapping results calculated at B3LYP/6-311G(d,p) level of theory for compound **1** and BHT are illustrated in Fig. 4. The nucleophilic and electrophilic sites are expressed in term of different color codes; a deep red color indicates an electron-rich site, whereas deep blue indicates an electron-deficient site. As presented in Fig. 4, the most electron-rich sites for compound **1** and BHT are located around the nitrogen and the oxygen atoms, respectively, whereas the most electron-deficient sites are one the hydrogen atoms of the hydrazone function and the phenolic hydroxyl group, respectively. These results confirm that the antioxidant properties of compound **1** and BHT are due to the hydrazone functions and the phenolic hydroxyl group, respectively.

## Acetylcholinesterase inhibitory activity

### In vitro acetylcholinesterase inhibitory activity

The capacity of the synthesized hydrazones **1–5** to inhibit *Electrophorus electricus* acetylcholinesterase (AChE) was evaluated using a modified Ellman's assay [28]. Galantamine (Gal.), used for mild Alzheimer's disease, was used as positive control. The obtained results are presented in Fig. 5 and Table S3 in SI. As can be seen, among the investigated hydrazones, compounds **1**, **2** and **3** have shown a moderate to excellent activity when compared to the galantamine. Compound **2**, bearing a methoxy group, is the best AChE inhibitor with an  $IC_{50}$  value ( $9.18 \pm 0.40 \mu\text{M}$ ) comparable to that of the galantamine ( $8.90 \pm 1.16 \mu\text{M}$ ). Compounds **4** and

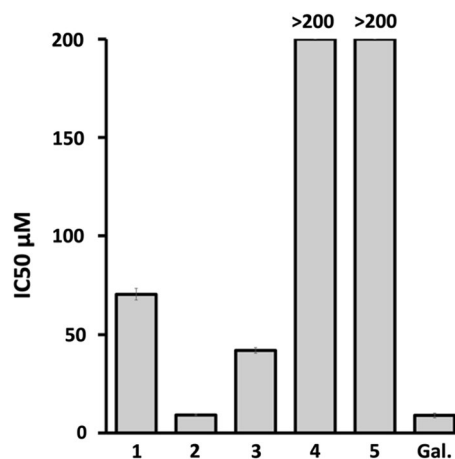


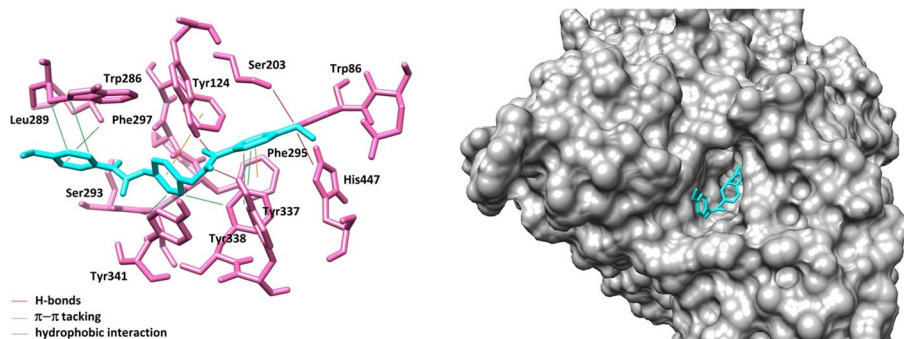
**Fig. 5**  $IC_{50}$  values for the inhibition of acetylcholinesterase for compounds **1–5** and galantamine

**5**, bearing, respectively, 4-Cl and 4-OCH<sub>2</sub>Ph, are the least reactive AChE inhibitors among the studied hydrazones, with  $IC_{50}$  values higher than 200  $\mu\text{M}$ . A comparison of the AChE inhibitory activity of hydrazones **1–5** with some data from the literature reveals that compound **2** is among the best AChE inhibitor of this family of compounds [65–67].

### Molecular docking study

Molecular docking studies are widely employed to explore the binding energy and to validate molecular mechanisms for ligands at the active site of a protein. In order to investigate the interaction modes of the synthesized hydrazones with AChE (PDB code: 1C2B), the most active compound (**2**) was subjected to molecular docking study using Blind Docking server. Figure 6 shows the most energetically favorable binding mode of compound **2** at the active site of AChE, and Table S4 in SI summarizes all the molecular docking binding interactions. To validate the approach used, we have also performed a molecular docking study for galantamine, and the obtained results for the most energetically favorable binding mode of this compound are tabulated in Table S5 in SI. The obtained results revealed that the most energetically favorable binding mode of compound **2** has a binding energy of  $-9.2 \text{ kcal/mol}$ . This energy is slightly lower than that obtained with galantamine ( $-8.30 \text{ kcal/mol}$ ). In this pose, compound **2** forms six hydrogen bonds, four bonds between the hydrazone functions and the residues Ser293, Tyr337 and Tyr124, and two bonds between the methoxy group and the residues His446 and Ser203. Also, the substituted aromatic moieties of compound **2** interact with Phe279, Trp86, Tyr337, Phe338, Phe295, Trp286 and Leu289 by weak  $\pi$ - $\pi$  stacking and hydrophobic interaction. Finally, the central aromatic nucleus forms hydrophobic interactions with Phe338 and Tyr341. Some of these residues are

**Fig. 6** Binding mode of compound **2** at the active site of AChE (PDB code: 1C2B)



reportedly involved in ligand–receptor complexes of tacrine, galantamine, huperzine A and donepezil [68]. From these results, it is clear that compound **2** possess a high binding affinity against acetylcholinesterase and can inhibit its activity, which is in good agreement with the experimental observations.

### Prediction of ADME parameters and BBB permeability

Good pharmacological activities are not enough for a compound to become a drug candidate. It is well known that absorption, distribution, metabolism and excretion (ADME) properties of a molecule are one of the main reasons of its failure in clinical trials [69]. After the evaluation of the antioxidant and acetylcholinesterase inhibitor activities of the synthesized hydrazones, we have studied their ADME properties by using Molinspiration online property calculation toolkit. All the obtained parameters are presented in Table 1. According to Lipinski's rule [70], in general, an orally active drug has no more than one violation of the following criteria: (1) No more than 5 hydrogen bond donors (n-OH/NH). (2) No more than 10 hydrogen bond acceptors (n-ON). (3) A molecular weight (MW) less than 500 D. (4) An octanol–water partition coefficient (milogP) not greater than 5. As shown in Table 1, all the tested hydrazones fitted Lipinski's rules by possessing no more than one violation, except compound **5** which showed two violations. In

addition, the percentage of absorption of the compounds has been calculated [71] and interesting values have been obtained for all the compounds (85.19–91.73%). Accordingly, it can be suggested that the synthesized hydrazones may be have a good pharmacokinetic profile and can be considered as drug candidates.

The BBB (blood–brain barrier) permeability is another important parameter that affects the biological activity results. Drugs that specifically target the central nervous system, such as cholinesterase inhibitors, must cross the blood–brain barrier. The BBB permeability of the synthesized hydrazones was evaluated by using the CBLigand-BBB prediction server, and the obtained results are presented in Table 1. The obtained results revealed that all the compounds are BBB-positive, which is required for the acetylcholinesterase activity.

### Conclusion

Five 1,4-bisphenylhydrazone derivatives have been synthesized and evaluated for their antioxidant and acetylcholinesterase inhibitory activities. All the compounds showed a very good antioxidant activity compared to the standards used. Among them, compound **1** proved to be the best antioxidant and compound **2** was the best inhibitor of acetylcholinesterase. From DFT calculation, the HAT mechanism was found to be the dominated mechanism in the gas phase, whereas

**Table 1** In silico some physicochemical and pharmacokinetic parameters of the synthesized 1,4-bisphenylhydrazone derivatives **1–5**

Comp.	miLogP <5	TPSA (°A)	MW <500	n-ON <10	n-OH/NH <5	n-rotb	MV	%ABS	vio. <1	BBB
<b>1</b>	7.59	48.78	314.39	4	2	6	298.19	91.73	1	+
<b>2</b>	7.70	67.25	374.44	6	2	8	349.28	85.19	1	+
<b>3</b>	8.81	48.78	370.50	4	2	6	364.43	91.73	1	+
<b>4</b>	8.66	48.78	383.28	4	2	6	325.26	91.73	1	+
<b>5</b>	9.36	67.25	526.64	6	2	12	492.58	85.19	2	+

%ABS percentage of absorption, TPSA topological polar surface area, n-rotb number of rotatable bonds, MW molecular weight, MV molecular volume, miLogP logarithm of partition coefficient between n-octanol and water, n-OH/NH number of hydrogen bond donors, n-ON number of hydrogen bond acceptors, vio Lipinski's violation, BBB blood–brain barrier permeability

the SPLET is the thermodynamically favorable pathway in ethanol. Finally, molecular docking study revealed a strong interaction between compound **2** and the active sites of AChE. In silico ADME studies have demonstrated that these compounds have a good pharmacokinetic profile.

**Acknowledgements** We would like to thank MESRS (Ministère de l'Enseignement Supérieur et de la Recherche Scientifique, Algeria) and DGRST (Direction Générale de la Recherche Scientifique et Technologique, Algeria) for financial support, as well as the HPC resources of UCI-UFMC (Unité de Calcul Intesif) of the university Frères Mentouri Constantine 1 for the computational resources used. We also thank Dr. Bensouici Chawki (Centre de recherche en Biotechnologie CRBt, Constantine, Algeria) for his help in the biological evaluation.

## References

- Xiang Y, Tong A, Jin P, Ju Y (2006) New fluorescent rhodamine hydrazone chemosensor for Cu(II) with high selectivity and sensitivity. *Org Lett* 8(13):2863–2866. <https://doi.org/10.1021/ol0610340>
- Patil DY, Patil AA, Khadke NB, Borhade AV (2019) Highly selective and sensitive colorimetric probe for Al<sup>3+</sup> and Fe<sup>3+</sup> metal ions based on 2-aminoquinolin-3-yl phenyl hydrazone Schiff base. *Inorg Chim Acta* 492:167–176
- Li Y, Wang C, Ma S, Zhang H, Ou J, Wei Y, Ye M (2019) Fabrication of hydrazone-linked covalent organic frameworks using alkyl amine as building block for high adsorption capacity of metal ions. *ACS Appl Mater Interfaces* 11(12):11706–11714
- Cappello D, Therien DAB, Staroverov VN, Lagugn -Labarthe F, Gilroy JB (2019) Optoelectronic, aggregation, and redox properties of double-rotor boron difluoride hydrazone dyes. *Chem A Eur J* 25(23):5994–6006
- Shen P, Liu X, Jiang S, Wang L, Yi L, Ye D, Zhao B, Tan S (2012) Synthesis of new N, N-diphenylhydrazone dyes for solar cells: effects of thiophene-derived  $\pi$ -conjugated bridge. *Dyes Pigments* 92(3):1042–1051
- Pouralimardan O, Chamayou A-C, Janiak C, Hosseini-Monfared H (2007) Hydrazone Schiff base-manganese (II) complexes: synthesis, crystal structure and catalytic reactivity. *Inorg Chim Acta* 360(5):1599–1608
- Nasr T, Bondock S, Youns M (2014) Anticancer activity of new coumarin substituted hydrazide-hydrazone derivatives. *Eur J Med Chem* 76:539–548
- Ajani OO, Obafemi CA, Nwinyi OC, Akinpelu DA (2010) Microwave assisted synthesis and antimicrobial activity of 2-quinoxalinone-3-hydrazone derivatives. *Bioorg Med Chem* 18(1):214–221
-  zkay Y, Tunalı Y, Karaca H, Işıkd ğ İ (2010) Antimicrobial activity and a SAR study of some novel benzimidazole derivatives bearing hydrazone moiety. *Eur J Med Chem* 45(8):3293–3298. <https://doi.org/10.1016/j.ejmech.2010.04.012>
- Debnath U, Mukherjee S, Joardar N, Babu SPS, Jana K, Misra AK (2019) Aryl quinolinyl hydrazone derivatives as anti-inflammatory agents that inhibit TLR4 activation in the macrophages. *Eur J Pharm Sci* 134:102–115
- Jia C, Yuan X, Liu X, Zhang L, Xiao Y, Fu B, Li J-Q, Qin Z (2019) Synthesis and fungicidal activity of (E)-methyl 2-(2-((1-cyano-2-hydrocarbylidenehydrazinyl)methyl)phenyl)-2-(methoxyimino)acetates. *Pest Manag Sci* 75(12):3160–3166. <https://doi.org/10.1002/ps.5432>
- Patole J, Sandbhor U, Padhye S, Deobagkar DN, Anson CE, Powell A (2003) Structural chemistry and in vitro antitubercular activity of acetylpyridine benzoyl hydrazone and its copper complex against *Mycobacterium smegmatis*. *Bioorg Med Chem Lett* 13(1):51–55
- El-Sabbagh OI, Rady HM (2009) Synthesis of new acridines and hydrazones derived from cyclic  $\beta$ -diketone for cytotoxic and antiviral evaluation. *Eur J Med Chem* 44(9):3680–3686
- Belkheiri N, Bouguerne B, Bedos-Belval F, Duran H, Bernis C, Salvayre R, N gre-Salvayre A, Baltas M (2010) Synthesis and antioxidant activity evaluation of a syringic hydrazones family. *Eur J Med Chem* 45(7):3019–3026
- Yılmaz AD, Coban T, Suzen S (2012) Synthesis and antioxidant activity evaluations of melatonin-based analogue indole-hydrazide/hydrazone derivatives. *J Enzyme Inhib Med Chem* 27(3):428–436
- Nastas  C, Tipericiu B, Duma M, Benedec D, Oniga O (2015) New hydrazones bearing thiazole scaffold: synthesis, characterization, antimicrobial, and antioxidant investigation. *Molecules* 20(9):17325–17338
- Puskullu MO, Shirinzadeh H, Nenni M, Gurer-Orhan H, Suzen S (2016) Synthesis and evaluation of antioxidant activity of new quinoline-2-carbaldehyde hydrazone derivatives: bioisosteric melatonin analogues. *J Enzyme Inhib Med Chem* 31(1):121–125
- Aruoma OI (1998) Free radicals, oxidative stress, and antioxidants in human health and disease. *J Am Oil Chem Soc* 75(2):199–212
- Jenner P (2003) Oxidative stress in Parkinson's disease. *Ann Neurol Off J Am Neurol Assoc Child Neurol Soc* 53(S3):S26–S38
- Kareem HS, Ariffin A, Nordin N, Heidelberg T, Abdul-Aziz A, Kong KW, Yehye WA (2015) Correlation of antioxidant activities with theoretical studies for new hydrazone compounds bearing a 3, 4, 5-trimethoxy benzyl moiety. *Eur J Med Chem* 103:497–505
- Peerannawar S, Horton W, Kokel A, T r k F, T r k M, T r k B (2017) Theoretical and experimental analysis of the antioxidant features of diarylhydrazones. *Struct Chem* 28(2):391–402
- Talesa VN (2001) Acetylcholinesterase in Alzheimer's disease. *Mech Ageing Dev* 122(16):1961–1969
- Blois MS (1958) Antioxidant determinations by the use of a stable free radical. *Nature* 181(4617):1199
- Re R, Pellegrini N, Proteggente A, Pannala A, Yang M, Rice-Evans C (1999) Antioxidant activity applying an improved ABTS radical cation decolorization assay. *Free Radic Biol Med* 26(9–10):1231–1237
- Apak R, G cl  K,  zy rek M, Karademir SE (2004) Novel total antioxidant capacity index for dietary polyphenols and vitamins C and E, using their cupric ion reducing capability in the presence of neocuproine: CUPRAC method. *J Agric Food Chem* 52(26):7970–7981. <https://doi.org/10.1021/jf048741x>
- Hyland K, Voisin E, Banoun H, Auclair C (1983) Superoxide dismutase assay using alkaline dimethylsulfoxide as superoxide anion-generating system. *Anal Biochem* 135(2):280–287. [https://doi.org/10.1016/0003-2697\(83\)90684-X](https://doi.org/10.1016/0003-2697(83)90684-X)
- Rhee IK, van de Meent M, Ingkaninan K, Verpoorte R (2001) Screening for acetylcholinesterase inhibitors from Amaryllidaceae using silica gel thin-layer chromatography in combination with bioactivity staining. *J Chromatogr A* 915(1):217–223. [https://doi.org/10.1016/S0021-9673\(01\)00624-0](https://doi.org/10.1016/S0021-9673(01)00624-0)
- Ellman GL, Courtney KD, Andres V, Featherstone RM (1961) A new and rapid colorimetric determination of acetylcholinesterase activity. *Biochem Pharmacol* 7(2):88–95. [https://doi.org/10.1016/0006-2952\(61\)90145-9](https://doi.org/10.1016/0006-2952(61)90145-9)
- Frisch MJ, Trucks G, Schlegel HB, Scuseria G, Robb M, Cheeseman J, Scalmani G, Barone V, Mennucci B, Petersson G (2009) Gaussian 09, revision A. 1. Gaussian Inc Wallingford CT 27:34

30. Becke AD (1988) Density-functional exchange-energy approximation with correct asymptotic behavior. *Phys Rev A* 38(6):3098
31. Hariharan PC, Pople JA (1973) The influence of polarization functions on molecular orbital hydrogenation energies. *Theor Chim Acta* 28(3):213–222. <https://doi.org/10.1007/bf00533485>
32. Mikulski D, Molski M (2010) Quantitative structure–antioxidant activity relationship of trans-resveratrol oligomers, trans-4,4'-dihydroxystilbene dimer, trans-resveratrol-3-O-glucuronide, glucosides: trans-piceid, cis-piceid, trans-astringin and trans-resveratrol-4'-O- $\beta$ -D-glucopyranoside. *Eur J Med Chem* 45(6):2366–2380. <https://doi.org/10.1016/j.ejmech.2010.02.016>
33. Praveena R, Sadasivam K, Deepha V, Sivakumar R (2014) Antioxidant potential of orientin: a combined experimental and DFT approach. *J Mol Struct* 1061:114–123. <https://doi.org/10.1016/j.molstruc.2014.01.002>
34. Praveena R, Sadasivam K, Kumaresan R, Deepha V, Sivakumar R (2013) Experimental and DFT studies on the antioxidant activity of a C-glycoside from *Rhynchosia capitata*. *Spectrochim Acta Part A Mol Biomol Spectrosc* 103:442–452. <https://doi.org/10.1016/j.saa.2012.11.001>
35. Boulebd H (2020) Comparative study of the radical scavenging behavior of ascorbic acid, BHT, BHA and Trolox: experimental and theoretical study. *J Mol Struct* 1201:127210. <https://doi.org/10.1016/j.molstruc.2019.127210>
36. Boulebd H (2019) DFT study of the antiradical properties of some aromatic compounds derived from antioxidant essential oils: C–H bond vs. O–H bond. *Free Radic Res* 53(11–12):1125–1134. <https://doi.org/10.1080/10715762.2019.1690652>
37. Rimarčík J, Lukeš V, Klein E, Ilčin M (2010) Study of the solvent effect on the enthalpies of homolytic and heterolytic N–H bond cleavage in p-phenylenediamine and tetracyano-p-phenylenediamine. *J Mol Struct (Theochem)* 952(1):25–30. <https://doi.org/10.1016/j.theochem.2010.04.002>
38. Thong NM, Duong T, Pham LT, Nam PC (2014) Theoretical investigation on the bond dissociation enthalpies of phenolic compounds extracted from *Artocarpus altilis* using ONIOM (ROB3LYP/6-311++G (2df, 2p): PM6) method. *Chem Phys Lett* 613:139–145
39. Thong NM, Quang DT, Bui NHT, Dao DQ, Nam PC (2015) Antioxidant properties of xanthenes extracted from the pericarp of *Garcinia mangostana* (Mangosteen): a theoretical study. *Chem Phys Lett* 625:30–35
40. Klein E, Rimarčík J, Lukes V (2009) DFT/B3LYP study of the O–H bond dissociation enthalpies and proton affinities of para- and meta-substituted phenols in water and benzene. *Acta Chim Slovaca* 2(2):37–51
41. Wright JS, Johnson ER, DiLabio GA (2001) Predicting the activity of phenolic antioxidants: theoretical method, analysis of substituent effects, and application to major families of antioxidants. *J Am Chem Soc* 123(6):1173–1183. <https://doi.org/10.1021/ja002455u>
42. Bartmess JE (1994) Thermodynamics of the electron and the proton. *J Phys Chem* 98(25):6420–6424. <https://doi.org/10.1021/j100076a029>
43. Parker VD (1992) Homolytic bond (H–A) dissociation free energies in solution. Applications of the standard potential of the (H+/H<sub>2</sub>) couple. *J Am Chem Soc* 114(19):7458–7462. <https://doi.org/10.1021/ja00045a018>
44. Bizarro Magda M, Cabral BJC, dos Santos RMB, Simões JAM (1999) Substituent effects on the O–H bond dissociation enthalpies in phenolic compounds: agreements and controversies + erratum. *Pure Appl Chem*. <https://doi.org/10.1351/pac199971071249>
45. Sánchez-Linares I, Pérez-Sánchez H, Cecilia JM, García JM (2012) High-throughput parallel blind virtual screening using BINDSURF. *BMC Bioinform* 13(14):S13
46. Pettersen EF, Goddard TD, Huang CC, Couch GS, Greenblatt DM, Meng EC, Ferrin TE (2004) UCSF Chimera—a visualization system for exploratory research and analysis. *J Comput Chem* 25(13):1605–1612
47. Huang D, Ou B, Prior RL (2005) The chemistry behind antioxidant capacity assays. *J Agric Food Chem* 53(6):1841–1856. <https://doi.org/10.1021/jf030723c>
48. Apak R, Güçlü K, Özyürek M, Çelik SE (2008) Mechanism of antioxidant capacity assays and the CUPRAC (cupric ion reducing antioxidant capacity) assay. *Microchim Acta* 160(4):413–419. <https://doi.org/10.1007/s00604-007-0777-0>
49. Zhang M, Dai Z-C, Qian S-S, Liu J-Y, Xiao Y, Lu A-M, Zhu H-L, Wang J-X, Ye Y-H (2014) Design, synthesis, antifungal, and antioxidant activities of (E)-6-(2-phenylhydrazono)methyl) quinoxaline derivatives. *J Agric Food Chem* 62(40):9637–9643. <https://doi.org/10.1021/jf504359p>
50. Török B, Sood A, Bag S, Tulsan R, Ghosh S, Borkin D, Kennedy AR, Melanson M, Madden R, Zhou W, LeVine H, Török M (2013) Diaryl hydrazones as multifunctional inhibitors of amyloid self-assembly. *Biochemistry* 52(7):1137–1148. <https://doi.org/10.1021/bi3012059>
51. Settypalli T, Chunduri VR, Maddineni AK, Begari N, Allagadda R, Kotha P, Chippada AR (2019) Design, synthesis, in silico docking studies and biological evaluation of novel quinoxaline-hydrazide hydrazone-1,2,3-triazole hybrids as  $\alpha$ -glucosidase inhibitors and antioxidants. *New J Chem* 43(38):15435–15452. <https://doi.org/10.1039/C9NJ02580D>
52. Prior RL, Wu X, Schaich K (2005) Standardized methods for the determination of antioxidant capacity and phenolics in foods and dietary supplements. *J Agric Food Chem* 53(10):4290–4302
53. Ames BN, Shigenaga MK, Hagen TM (1993) Oxidants, antioxidants, and the degenerative diseases of aging. *Proc Natl Acad Sci USA* 90(17):7915–7922
54. Wang G, Xue Y, An L, Zheng Y, Dou Y, Zhang L, Liu Y (2015) Theoretical study on the structural and antioxidant properties of some recently synthesised 2,4,5-trimethoxy chalcones. *Food Chem* 171:89–97. <https://doi.org/10.1016/j.foodchem.2014.08.106>
55. Estévez L, Otero N, Mosquera RA (2010) A computational study on the acidity dependence of radical-scavenging mechanisms of anthocyanidins. *J Phys Chem B* 114(29):9706–9712. <https://doi.org/10.1021/jp1041266>
56. Zheng Y-Z, Deng G, Guo R, Fu Z-M, Chen D-F (2019) Theoretical insight into the antioxidative activity of isoflavonoid: the effect of the C2=C3 double bond. *Phytochemistry* 166:112075. <https://doi.org/10.1016/j.phytochem.2019.112075>
57. Zheng Y-Z, Deng G, Liang Q, Chen D-F, Guo R, Lai R-C (2017) Antioxidant activity of quercetin and its glucosides from propolis: a theoretical study. *Sci Rep* 7(1):7543
58. Xue Y, Liu Y, Zhang L, Wang H, Luo Q, Chen R, Liu Y, Li Y (2019) Antioxidant and spectral properties of chalcones and analogous aurones: theoretical insights. *Int J Quantum Chem* 119(3):e25808. <https://doi.org/10.1002/qua.25808>
59. Shang Y, Zhou H, Li X, Zhou J, Chen K (2019) Theoretical studies on the antioxidant activity of viniferifuran. *New J Chem* 43(39):15736–15742. <https://doi.org/10.1039/C9NJ02735A>
60. Xue Y, Zheng Y, An L, Dou Y, Liu Y (2014) Density functional theory study of the structure–antioxidant activity of polyphenolic deoxybenzoins. *Food Chem* 151:198–206. <https://doi.org/10.1016/j.foodchem.2013.11.064>
61. Trouillas P, Marsal P, Siri D, Lazzaroni R, Duroux J-L (2006) A DFT study of the reactivity of OH groups in quercetin and taxifolin antioxidants: the specificity of the 3-OH site. *Food Chem* 97(4):679–688
62. Sadasivam K, Kumaresan R (2011) Antioxidant behavior of mearnsenin and myricetin flavonoid compounds—a DFT study.

- Spectrochim Acta Part A Mol Biomol Spectrosc 79(1):282–293. <https://doi.org/10.1016/j.saa.2011.02.042>
63. Politzer P, Laurence PR, Jayasuriya K (1985) Molecular electrostatic potentials: an effective tool for the elucidation of biochemical phenomena. *Environ Health Perspect* 61:191–202. <https://doi.org/10.1289/ehp.8561191>
  64. Rajan VK, Muraleedharan K (2017) A computational investigation on the structure, global parameters and antioxidant capacity of a polyphenol, Gallic acid. *Food Chem* 220:93–99. <https://doi.org/10.1016/j.foodchem.2016.09.178>
  65. Karaman N, Sıcak Y, Taşkın-Tok T, Öztürk M, Karaküçük-İyidoğan A, Dikmen M, Koçyiğit-Kaymakçioğlu B, Oruç-Emre EE (2016) New piperidine-hydrazone derivatives: synthesis, biological evaluations and molecular docking studies as AChE and BChE inhibitors. *Eur J Med Chem* 124:270–283. <https://doi.org/10.1016/j.ejmech.2016.08.037>
  66. Petronilho E, Rennó M, Castro NG, da Silva FMR, Pinto A, Figueroa-Villar JD (2016) Design, synthesis, and evaluation of guanylhydrazones as potential inhibitors or reactivators of acetylcholinesterase. *J Enzyme Inhib Med Chem* 31(6):1069–1078. <https://doi.org/10.3109/14756366.2015.1094468>
  67. Tripathi RKP, Ayyannan SR (2018) Evaluation of 2-amino-6-nitrobenzothiazole derived hydrazones as acetylcholinesterase inhibitors: in vitro assays, molecular docking and theoretical ADMET prediction. *Med Chem Res* 27(3):709–725. <https://doi.org/10.1007/s00044-017-2095-3>
  68. Cheung J, Rudolph MJ, Burshteyn F, Cassidy MS, Gary EN, Love J, Franklin MC, Height JJ (2012) Structures of human acetylcholinesterase in complex with pharmacologically important ligands. *J Med Chem* 55(22):10282–10286. <https://doi.org/10.1021/jm300871x>
  69. Li AP (2001) Screening for human ADME/Tox drug properties in drug discovery. *Drug Discovery Today* 6(7):357–366
  70. Lipinski CA, Lombardo F, Dominy BW, Feeney PJ (1997) Experimental and computational approaches to estimate solubility and permeability in drug discovery and development settings. *Adv Drug Deliv Rev* 23(1–3):3–25
  71. Zhao YH, Abraham MH, Le J, Hersey A, Luscombe CN, Beck G, Sherborne B, Cooper I (2002) Rate-limited steps of human oral absorption and QSAR studies. *Pharm Res* 19(10):1446–1457

**Publisher's Note** Springer Nature remains neutral with regard to jurisdictional claims in published maps and institutional affiliations.

## Affiliations

Imene Amine Khodja<sup>1</sup> · Housseem Boulebd<sup>1</sup> 

✉ Housseem Boulebd  
boulebd.housseem@umc.edu.dz

<sup>1</sup> Laboratory of Synthesis of Molecules with Biological Interest, University of Frères Mentouri Constantine 1, Constantine, Algeria